ISSN 1648-7788 / eISSN 1822-4180

VILNIUS TECH
Vilnius Gediminas Technical University

AVIATION

2024
Volume 28
Issue 4
Pages 206–214
https://doi.org/10.3846/aviation.2024.22577

SIMULATION AND EVALUATION OF LATERAL/DIRECTIONAL DYNAMICS IN AN AIRCRAFT AUTOPILOT CONTROL SYSTEM

Carlos SÁNCHEZ [1]✉, Mildred CAJAS [2], Paola CALVOPIÑA [2], Andrés ORTEGA [3]

[1]*Departamento de Ciencias de la Energía y Mecánica, Universidad de las Fuerzas Armadas ESPE, Sangolquí, Ecuador*
[2]*Departamento de Eléctrica y Electrónica, Universidad de las Fuerzas Armadas ESPE, Sangolquí, Ecuador*
[3]*Departamento de Ciencias Exactas, Universidad de las Fuerzas Armadas ESPE, Sangolquí, Ecuador*

Article History:
- received 21 May 2024
- accepted 10 September 2024

Abstract. The objective of the research was to design and simulate the lateral/directional dynamics control of an aircraft's autopilot system to automate the landing approach execution, complying with the requirements of the Instrument Landing System (CAT III C). The design methodology involved integrating a Linear Quadratic Regulator (LQR) with Affine Parameterization techniques to create a robust control system. The prototype was developed using Matlab and simulated in Simulink. Through various simulations, adjustments were made to the Q and R matrices of the LQR controller based on Bryson's rule, allowing the system to adapt to the nonlinearities and dynamic constraints of the aircraft model. These adjustments included modifying the lateral attitude control parameters to achieve the desired damping factors and time constants, ensuring flight quality standards according to MIL-8785C. Validation under real conditions through a flight simulator confirmed the control system's effectiveness under various operational conditions. The controllers are able to maintain the aircraft's alignment with the runway centerline, even in the presence of external disturbances, thus demonstrating the system's robustness and reliability. The methodologies and results provide a solid foundation for future improvements and comparative analyses of autopilot systems within CAT III C requirements.

Keywords: lateral/directional dynamics, autopilot system, instrument landing system (ILS), linear quadratic regulator (LQR), affine parameterization, flight simulator validation.

✉Corresponding author. E-mail: *crsanchez9@espe.edu.ec*

1. Introduction

The aviation industry is experiencing steady growth, driven by the demand for more efficient and safer flights (Afonso et al., 2023). Automatic aircraft control is a highly developed area within aeronautical engineering, particularly in the design of robust autopilots capable of ensuring safety and stability during the most critical phases of flight, such as instrument landings under low-visibility conditions (Collinson, 2023). These conditions, classified under instrument landing categories, present varying levels of difficulty, with CAT III C being the most demanding. In this category, landing is conducted solely using flight instruments, with no visual references (Coello et al., 2023), and the control system must guide the aircraft with extreme precision until runway contact.

In recent decades, advances in control theory have allowed the development of more efficient and robust algorithms that guarantee optimum performance in these critical phases (Simões & Cavalcanti, 2023). Among these advances, predictive and optimization algorithms stand out, which have proven to be effective tools for solving problems in real time, handling disturbances and uncertainties inherent to the operating environment (Cortez et al., 2020). However, there are still technical challenges that require further research, such as the ability of controllers to adapt to abrupt changes in flight conditions and the need to reduce computational complexity for real-time applications (Alabsi & Fields, 2018).

The present study aims to develop and optimize a lateral/directional control system for an aircraft, specifically designed to meet the stringent requirements for operation in CAT III C landing conditions (Coello et al., 2023). The design focuses on the use of Affine Parameterization techniques in conjunction with a Linear Quadratic Regulator (LQR), widely recognized for its ability to balance optimal performance with system stability (Rodrigues, 2021). However, advanced optimization techniques, such as Bryson's rule (Sir & Naci, 2022), are applied to adjust the weights in the cost function of the LQR, allowing greater robustness of the controller to external disturbances (Benevides et al., 2022).

In the field of automation and control, recent advances in optimization and predictive control algorithms have significantly improved the accuracy and robustness of automated systems (Sir & Naci, 2022). Recent studies have demonstrated how a cooperative optimization algorithm can enhance trajectory tracking in robotic manipulators, with applications to complex dynamic systems such as aircraft control systems (Elsisi et al., 2021). This technique reduces trajectory errors and increases accuracy in environments where conditions change rapidly (Azeez et al., 2023). Similarly, advanced predictive models have been developed for aircraft flight control, utilizing intelligent techniques to enhance stability in adverse conditions (Elbatal et al., 2021). This approach, based on artificial intelligence, enables the control system to anticipate disturbances before they occur (Zuo et al., 2022), proactively adjusting system parameters to maintain aircraft stability (Mo & Farid, 2019).

In terms of robustness against uncertain conditions, a robust Kalman filter has been proposed for accurate position estimation of automatically guided vehicles, even under cyber-attacks (Elsisi et al., 2023). This approach is relevant to aircraft control, given the need to maintain high accuracy in position and orientation estimation during landing. The combination of robust optimization techniques with adaptive Kalman filters has proven to be an effective solution for improving the reliability of control systems (Reis et al., 2023). Recent studies have developed models with low computational load using the Dandelion optimization algorithm, designed for autonomous vehicles (Liu & Qin, 2020). This algorithm is notable for its ability to manage the uncertainty of vision systems, with direct applications in the control of aircraft operating under low visibility conditions. The low computational load of these algorithms is especially important for real-time implementation, where computational resources are limited and a fast system response is required (Zhao et al., 2022).

The present study advances current research in aircraft control by developing a controller based on Linear Quadratic Regulator (LQR) theory, which is tuned using advanced optimization techniques to enhance the stability and robustness of the system (Sir & Naci, 2022). Unlike previous studies, this approach specifically targets the optimization of aircraft lateral and directional dynamics during the critical landing phase by employing Affine Parameterization techniques to ensure compliance with operational requirements in real-world scenarios (Cavanini et al., 2021). The validation of this approach is conducted through detailed simulations that replicate real flight conditions under CAT III C. The results demonstrate a significant improvement in lateral and directional alignment accuracy compared to traditional control methods, such as computationally intensive predictive algorithms. This work not only enhances aircraft control under critical conditions but also offers a more efficient and robust solution by utilizing advanced optimization and control techniques, which can be applied to a broad range of autonomous systems.

2. Automatic Landing System (ILS)

2.1. The Instrument Landing System

Two radio beams are used by the Instrument Landing System (ILS), a precision approach tool, to give pilots vertical and horizontal direction during approach and landing (Aishwarya, 2022). While the glide slope (GS) establishes the appropriate vertical descent profile, the localizer (LOC) offers azimuthal guidance. High-intensity runway lights and marker beacons are further possible ILS use assistance. As visible in Figure 1, the LOC antennas are typically situated at the end of the runway. They broadcast two narrow intersecting beams, one pointing slightly to the left and the other to the right of the runway's center, which together create the "on LOC" indicator. As seen in Figure 2, the GS antennas broadcast two narrow beams that cross at a point where they define the "on GS" indication at the airplane. One of the narrow beams intersects just below the required vertical profile, and the other slightly above it (Coello et al., 2023).

The highest ILS category, CAT III C, permits fully autonomous landing in both overhead and zero visibility situations. In this category, there are no minimum requirements. The aircraft is landed and decelerated by the autopilot (A/P) until the pilot takes over and deactivates the A/P to remove the aircraft from the runway. An automatic landing system that can intercept the glide slope and localizer signals as previously mentioned is needed to land an aircraft without a visual reference to the runway (Coello et al., 2023). The aircraft is then guided along the glide slope at a specific rate of descent until it reaches a height at which it performs the flare maneuver to touch the runway (Dudek & Kozłowski, 2018).

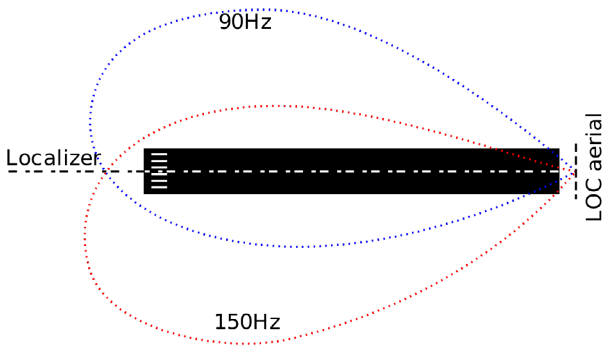

Figure 1. Aircraft on the best route for a localizer (LOC)

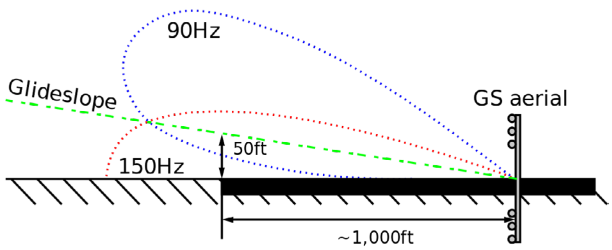

Figure 2. Aircraft on the best glide slope (GS) trajectory

3. Mathematical model of lateral/directional dynamics

Accurate control of the lateral and directional dynamics of an aircraft is essential to ensure its stability and maneuverability, especially in critical situations such as landing in low visibility conditions. The mathematical representation of this behavior is fundamental to develop efficient controllers that can handle external disturbances and meet the constraints imposed by the inherent dynamics of the aircraft.

3.1. Aircraft model

The mathematical model of an aircraft follows the classic approach of flight dynamics, which is divided into longitudinal and lateral/directional dynamics. This work focuses on the lateral/directional dynamics, describing the movements related to yaw, roll, and sideslip. To capture these movements, state equations are developed based on the forces and moments acting on the aircraft. These equations are formulated using Newton-Euler laws, where the nonlinear equations of motion are linearized around a specific operating point by analyzing small perturbations from a steady flight condition. The state-space representation, linking input variables (control surface deflections) with output variables (yaw angle, roll angle, and lateral velocity), allows the design of controllers based on optimal control technique (see Figure 3).

Aerodynamic transfer functions describe the fundamental relationships between control inputs and the aircraft's flying characteristics, and they can account for atmospheric disturbances when necessary (American Institute of Aeronautics and Astronautics [AIAA], 2000). These correlations are expressed through a state equation, which represents the aircraft's equations of motion as a first-order vector differential equation (Coello et al., 2023). The general form of this equation is shown in Eq. (1), where $\{x(t)\}$ is the state vector and $\{u(t)\}$ is the control vector. State variables are the elements of vector $\{x(t)\}$, while control input variables are the components of vector $\{u(t)\}$. The input matrix is [B], while the state matrix is [A]. More information about the system of equations governing the aircraft's motion may be found in Sun and Adnan (2021).

$$\{\dot{x}(t)\} = [A]\{x(t)\} + [B]\{u(t)\}. \quad (1)$$

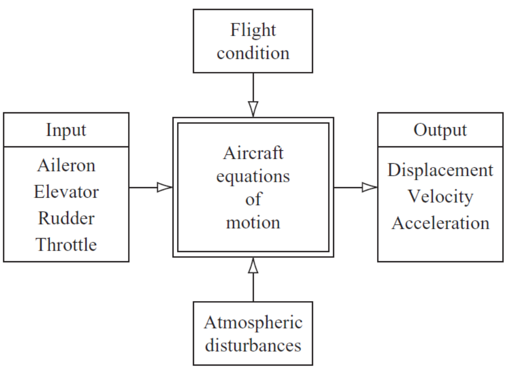

Figure 3. Basic control – response relationships

3.2. Lateral/directional dynamics model

The lateral/directional dynamics model describes how aerodynamic forces and moments affect the stability and control in the lateral and yaw axes. These aerodynamic forces mainly originate from differential lift on the wings, the interaction of ailerons, rudder, and fuselage with airflow, as well as engine thrust.

The methods used to interpret an aircraft's lateral/directional dynamics are quite similar to those used in longitudinal dynamics (Coello et al., 2023). The primary distinction in solving the equations lies in the additional algebra required, since, as shown in Figure 4, two aerodynamic inputs, the rudder ζ and the ailerons ξ, are involved. Because most aircraft are designed with aerodynamic symmetry, lateral/directional dynamics are less affected by flying conditions than longitudinal dynamics (Cook, 2013).

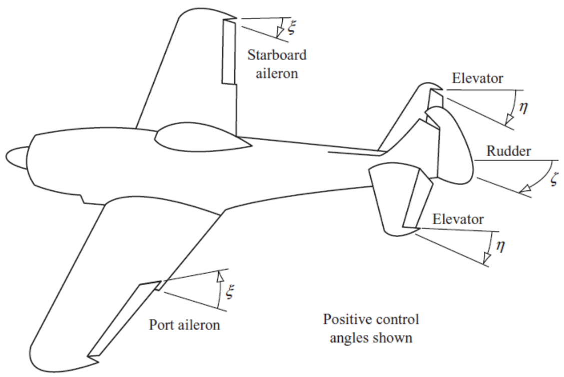

Figure 4. Aerodynamic controls notation

Eq. (2) provides the lateral/directional motion equations, which are derived from the equation of state Eq. (1) and represent small perturbations around an equilibrium condition with respect to the wind axes (Cook, 2013). v represents the disturbance in lateral velocity, p, r, ϕ, ξ, and ζ, respectively, represent roll rate, yaw rate, roll angle, aileron angle, and rudder angle perturbations. Additionally, the definitions of the derivatives are provided in Cook (2013). The coefficients of the input matrix [B] are the lateral control derivatives, while the coefficients of the state matrix [A] are the lateral aerodynamic stability derivatives.

$$\begin{Bmatrix} \dot{v} \\ \dot{p} \\ \dot{r} \\ \dot{\phi} \end{Bmatrix} = \begin{bmatrix} y_v & y_p & y_r & y_\phi \\ l_v & l_p & l_r & l_\phi \\ n_v & n_p & n_r & n_\phi \\ 0 & 1 & 0 & 0 \end{bmatrix} \begin{Bmatrix} v \\ p \\ r \\ \phi \end{Bmatrix} + \begin{bmatrix} y_\xi & y_\zeta \\ l_\xi & l_\zeta \\ n_\xi & n_\zeta \\ 0 & 0 \end{bmatrix} \begin{Bmatrix} \xi \\ \zeta \end{Bmatrix}. \quad (2)$$

4. Dynamic model of direction and lateral motion

The dynamic model of the lateral and directional motion is based on the linearized approximation of the system, focusing on the aerodynamic derivatives and the effects of lateral forces and moments on the aircraft. This allows a simplified representation that facilitates the design and analysis of the controllers. Both the lateral attitude and the lateral trajectory controllers make up the control system for coupling to the runway axis (localizer). Together, these allow the aircraft to make the necessary movements to achieve a precise lateral attitude (roll) and lateral trajectory (heading) during the approach phase, until intercepting the runway center line (localizer).

During the optimization process of the control model, restrictions are applied to ensure system safety and operability. These include the physical limits of control surfaces (ailerons and rudder) and the aerodynamic characteristics of the aircraft. These restrictions are integrated into the system's equations to prevent the controller from exceeding the aircraft's capabilities. Through predictive control techniques, control inputs are adjusted in real-time, ensuring efficient and stable operation under varying conditions, while minimizing tracking errors and respecting physical and dynamic limits.

Figure 5 shows the variables involved in coupling the aircraft to the localizer. The aircraft must attempt to follow the flight path (beam center-line), where d indicates the lateral distance of the aircraft off course. ψ_{ref} represents the heading set by the pilot, while $(\psi - \psi_{ref})$ is the course angle that the aircraft must follow. The lateral distance of the aircraft off course d increases as a function of the course angle, as indicated in Eq. (3), where ψ is also a function of the roll angle ϕ and is defined by the expression in Eq. (4).

$$\dot{d}(t) = U_0 \sin\left(\psi\left(t\right) - \psi_{ref}\right) \approx U_0\left(\psi\left(t\right) - \psi_{ref}\right); \tag{3}$$

$$\dot{\psi}(t) = \frac{1}{U_0} g \sin\left(\phi\left(t\right)\right) \approx \frac{g}{U_0}\phi\left(t\right). \tag{4}$$

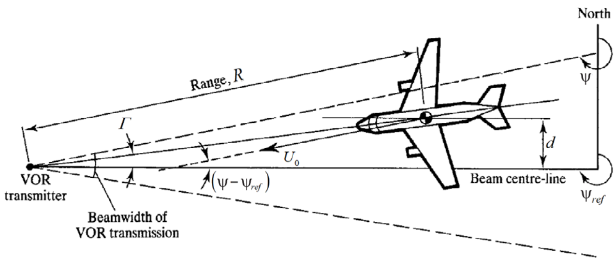

Figure 5. Terminology in coupling the aircraft to the localizer

Once the localizer is intercepted, the rolling attitude must be controlled and the speed U_0 is assumed constant, which is regulated by the speed controller integrated into the longitudinal dynamics (Coello et al., 2023). The usual beamwidth of the VOR transmission angle is 2.5°, and the distance R represents the aircraft's distance from the VOR station.

4.1. Controller of lateral attitude

Using the Multiple-Input Multiple-Output (MIMO) concept and the LQR approach, the lateral attitude controller was created, the procedure is detailed in Cook (2013) and Guardeño et al. (2019). Since it is believed that the whole state is quantifiable, an observer is not required when designing the roll or lateral attitude controller. It is also common to express the lateral velocity perturbation v in Eq. (2) in terms of the lateral slip angle β, since for small perturbations $v = \beta U_0$ obtaining Eq. (5).

$$\begin{Bmatrix} \dot{\beta} \\ \dot{p} \\ \dot{r} \\ \dot{\phi} \end{Bmatrix} = \begin{bmatrix} y_v & y_p / U_0 & y_r / U_0 & y_\phi / U_0 \\ l_v U_0 & l_p & l_r & l_\phi \\ n_v U_0 & n_p & n_r & n_\phi \\ 0 & 1 & 0 & 0 \end{bmatrix} \begin{Bmatrix} \beta \\ p \\ r \\ \phi \end{Bmatrix} + \begin{bmatrix} y_\xi / U_0 & y_\zeta / U_0 \\ l_\xi & l_\zeta \\ n_\xi & n_\zeta \\ 0 & 0 \end{bmatrix} \begin{Bmatrix} \xi \\ \zeta \end{Bmatrix}. \tag{5}$$

The lateral modes provided by the state matrix may be seen based on the aircraft's open loop dynamics. The roll subsidence mode (fast mode) with a time constant of T_r = 1.15 s, the dutch roll mode (oscillatory mode) with a frequency of ω_d = 0.67 rad / s and a damping factor of ς_d = 0.0345, and the spiral mode (slow mode) with a time constant of T_s = 44.9 s were found. The dutch roll had some damping, thus it was required to employ closed loop control to enhance the damping. To do this, the aircraft's MIL-8785C standard flight quality standards were followed, as shown in Cook (2013) and Fu et al. (2020). Furthermore, for the disturbance limits of the aileron deflection ± 32° (± 1 normalized) and the rudder ± 20° (± 1 normalized) were considered.

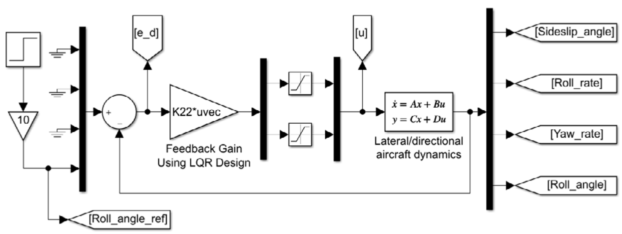

Figure 6. The lateral attitude controller block diagram

Bryson's principles, as described in Okyere et al. (2019) and Kashyap and Vepa (2023), were used to create the Q and R matrices. The LQR approach was then used to adjust the matrices' coefficients until the desired closed loop characteristics were achieved. Thus, it was possible to determine the time constants for the spiral mode T_s = 0.49 s, roll subsidence mode T_r = 0.28 s, frequency of dutch roll mode ω_d = 2.85 rad / s and damping factor ς_d = 0.71. After the roll or lateral attitude controller was created as shown in Figure 6, its functionality was tested using a simulation for a step reference of the roll angle of the aircraft.

4.2. Controller of lateral trajectory

Using the Single-Input Single-Output (SISO) concept and Affine Parameterization, the lateral trajectory controller was created. Considering that the lateral attitude control designed in the previous point is fast enough compared to the lateral trajectory control, the lateral trajectory control system was designed and a simulation was utilized to confirm that it functions as intended, the model for trajectory control lateral is defined by Eq. (6), where $d(s)$ is the expression that indicates the lateral distance of the aircraft off course, $\phi(s)$ is the expression of the roll angle depending on the variable s, the value of gravity's acceleration is expressed as g.

$$G_{012} = \frac{d(s)}{\phi(s)} = \frac{g}{s}. \tag{6}$$

A lower limit was found for the frequency provided by the gusts to which the aircraft is subjected, and a frequency of 0.30 *rad / s* was specified for the lateral trajectory controller. For this, a Dryden turbulence model was proposed (Qiao & Wu, 2023). Thus, for the lateral velocity, a spectral analysis was carried, where it is observed that the lower limit of the frequency is 0.35 *rad / s*, therefore, said value was chosen for an establishment time of approximately 15 seconds.

$$F_Q(s) = \frac{\alpha_2 s^2 + \alpha_1 s + 1}{\alpha_4 s^4 + \alpha_3 s^3 + \alpha_2 s^2 + \alpha_1 s + 1}. \tag{7}$$

Next, in order to compel the integral action in the controller, the desired complementary sensitivity function $F_Q(s)$ was developed. In addition, it was taken into account that the plant has two integrators, the relative degree of the open loop is 2 (Sariyildiz & Ohnishi, 2015), therefore, the closed loop must have at least the same relative degree as the open loop, for the controller $K_{12}(s)$ to be a biproper function as seen in Eq. (7). Having forced the integral action in the controller, it was necessary to include an anti-windup scheme through output feedback, which requires that the controller be biproper and have minimum phase. After the vertical trajectory controller was created (see Figure 7), its functionality was tested using a simulation for a step reference of the lateral distance of the aircraft off course d.

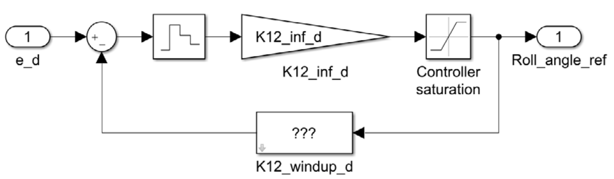

Figure 7. The lateral trajectory controller block diagram

5. Integration, verification, and outcome analysis

Under ideal circumstances, unit tests were conducted on the controllers that had previously been created. However, it was essential to experimentally validate them under real operating conditions to ensure that they were able to interact and achieve the desired control action in each situation. These controllers were included in a dynamic autopilot simulation model developed in Matlab/Simulink, the same one that simulates the real aircraft. Figure 8 illustrates how the controllers with their corresponding architectures were incorporated into the Flight Control Computer (FCC), and Figures 9 and 10 demonstrate how each controller was implemented.

The selection of the proposed algorithm's parameters was carried out through an iterative process that considered both system stability and performance under typical operating conditions. Initially, reference values were established based on previous studies and existing literature. These values were progressively adjusted through simulations that evaluated the system's response to different flight scenarios, including disturbances and variations in atmospheric conditions. During this process, multi-objective optimization techniques were used to balance trajectory tracking accuracy and system robustness.

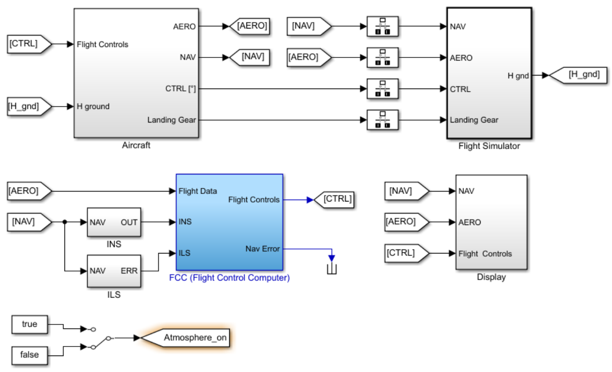

Figure 8. Dynamic autopilot simulation model

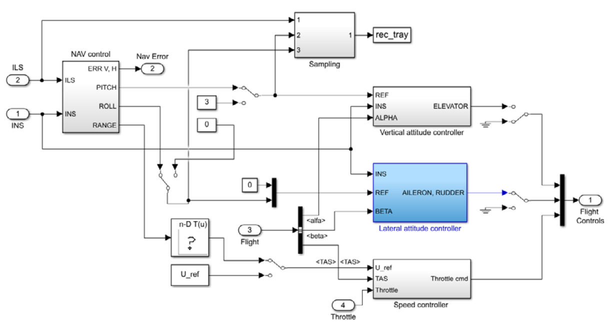

Figure 9. Integration of lateral attitude controller in the FCC, ILS autoland

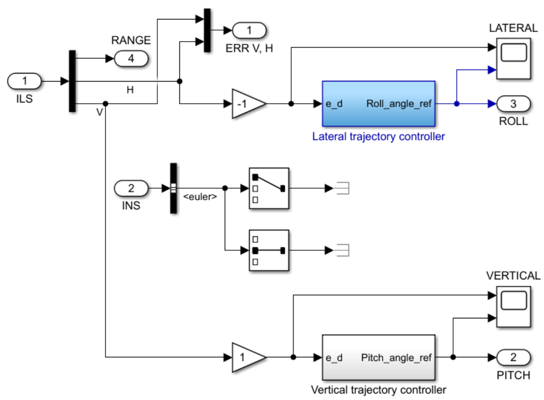

Figure 10. Integration of lateral trajectory controller in the FCC, ILS autoland

The lateral trajectory controller was evaluated in straight and level flight after the controllers were included into a dynamic autopilot simulation model created in Matlab/Simulink, the same model that replicates the behavior of the actual airplane. Figure 11 indicates a settling time of around 22 seconds for an initial aircraft lateral off-course distance of 5.3 meters, whereas the design time was about 18 seconds. The aircraft's response is acceptable as long as there is a minimum of a decade between the lateral attitude controller and the lateral trajectory controller. This is because of the limitations placed by the lateral trajectory model. Figure 12 shows how the aircraft speed, roll angle and control action vary.

Next, under ideal circumstances, the lateral trajectory controller was tested to couple to the runway localizer. Figure 13 illustrates how the aircraft couples to the runway axis (localizer) by displaying the aircraft's range *R* until it reaches the runway and the tracking error for the initial lateral distance of the aircraft off course *d*, as previously analyzed. However, Figure 14 illustrates how the aircraft maintains a constant speed until about second 28, at which point it is thought to have reached the decision height and the flare control system is turned on to facilitate the aircraft's transition from decision height to the runway. The speed control is observed to decrease with a constant roll angle, suggesting that the aircraft maintains its alignment with the runway.

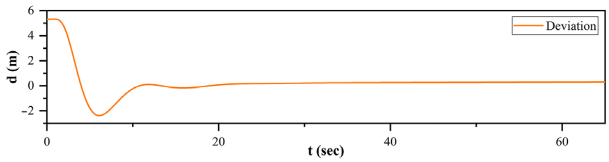

Figure 11. Test of lateral trajectory controller, d = 5.3 m

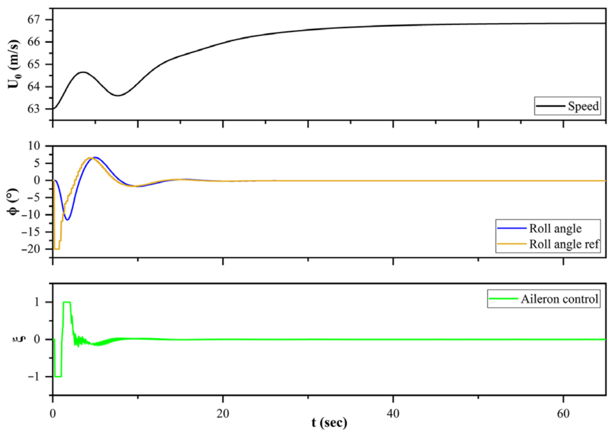

Figure 12. Test of lateral attitude controller, d = 5.3 m

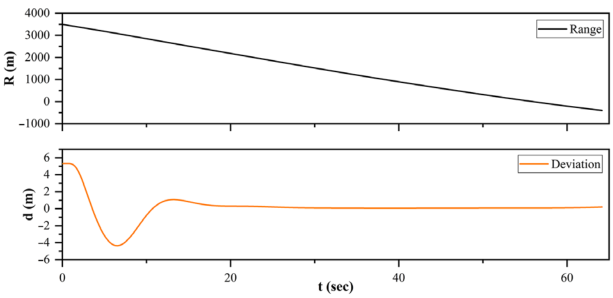

Figure 13. Test of lateral trajectory controller, localizer coupling with ideal conditions

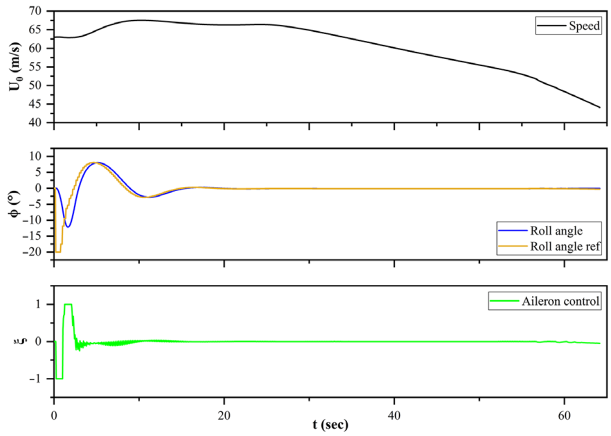

Figure 14. Test of lateral attitude controller, localizer coupling with ideal conditions

After that, a real-world condition coupling test of the lateral trajectory controller to the runway localizer was performed. Figure 15 shows the aircraft's range *R* until it reaches the runway as well as the tracking error for the off-course lateral distance *d*, which exhibits more fluctuations in this instance. Due to disturbances, the answer is not as clear as it would be in an ideal scenario. Similar to Figure 16, which depicts how the speed stays nearly constant until about second 20, the flare control system activates for the transition from that level height to the runway, and it is assumed that the aircraft has reached the decision height. This is where you can see that the aircraft maintains the runway axis because the roll angle is nearly constant and the speed control is reducing the aircraft's velocity. It is important to emphasize the numerous fluctuations that this control action in this instance presents.

To evaluate the robustness of the proposed model, extensive tests were conducted under various turbulence conditions and atmospheric disturbances. The analysis included simulations replicating different levels of turbulence

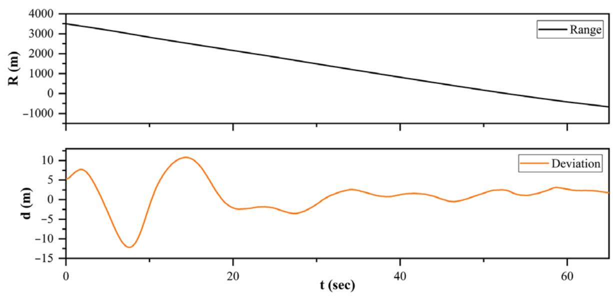

Figure 15. Test of lateral trajectory controller, localizer coupling with real conditions

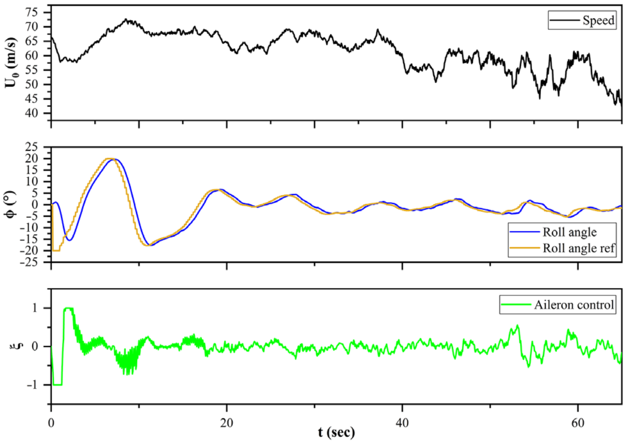

Figure 16. Test of lateral attitude controller, localizer coupling with real conditions

Figure 17. Aircraft flight simulator

and changes in flight conditions, such as variations in wind speed and altitude. The results showed that the model maintained robust and stable performance, with effective capability to adjust control inputs and minimize errors in the desired trajectory.

A predictive control approach was used to anticipate and manage disturbances, and the results indicated that the model managed to maintain system stability within an acceptable range of extreme conditions. The system's response was evaluated in terms of its ability to follow the desired trajectory and its resistance to external disturbances, demonstrating that the controller performed effectively within the limits defined by physical and operational constraints.

However, it was observed that performance could be affected by severe turbulence and sudden changes in atmospheric conditions, suggesting the need for future improvements in the algorithm's adaptation for even more adverse flight scenarios. This robustness analysis validated the model's effectiveness under controlled conditions and highlighted the importance of continuing to develop techniques to enhance system stability and accuracy in real-world flight environments.

In the end, the controllers were tested and put into use by programming codes in a flight simulator (see Figure 17). In Figure 18 you can see how the aircraft docks to the runway center line (localizer), and then automatically executes an approach and landing circuit, as shown in Figure 19. This final step in the development process and test demonstrates the effectiveness and precision of the controllers in simulated flight situations.

Figure 18. Aircraft docking to the runway axis (localizer)

Figure 19. Automatic execution of approach and landing

6. Conclusions

The effectiveness of the autopilot system in controlling the aircraft's lateral/directional dynamics is demonstrated through its implementation and simulation. This system shows solid and acceptable performance, particularly in the automatic execution of approach and landing circuits according to Category III C Instrument Landing System standards.

Adjustments made to the controller parameters have allowed for the absorption of constraints imposed by the aircraft model, thereby enhancing the system's robustness. The optimization of controller parameters using sophisticated techniques such as Affine Parameterization and the Linear Quadratic Regulator (LQR) has achieved adjustments in the closed-loop response characteristics, applying Bryson's rules to vary the coefficients of the Q and R matrices.

The incorporation of integral action in the lateral trajectory controller ensures precise and stable response, eliminating error at low frequencies, which is crucial in challenging flight situations requiring precise trajectory correction. The validation of the designed controllers has been carried out comprehensively, using both simulations in controlled environments and tests in real operational situations. This approach ensures the effectiveness and accuracy of the control system under various flight conditions and scenarios, supporting its successful implementation in practical applications.

Despite positive results, there are significant limitations to the practical implementation of the proposed model. Major challenges include the computational capacity required to run the algorithm in real-time, especially under significant atmospheric variations and external disturbances. The system's response time could be compromised in aircraft with low-capacity onboard control systems. Additionally, the maximum deflections of control surfaces imposed by physical constraints may limit the controller's ability to make rapid and precise adjustments, affecting the system's robustness under extreme conditions. These limitations should be addressed in future studies through the optimization of control hardware and fine-tuning of the algorithm to improve its performance in real-world applications.

To advance the development of aircraft control systems, several research areas are recommended. First, exploring adaptive control algorithms that dynamically respond to real-time atmospheric changes could be beneficial. Second, studying robust control techniques that handle more severe disturbances and extreme flight condition variations might further enhance the system's ability to operate in more challenging environments. Additionally, developing and testing control systems with more advanced real-time data processing capabilities could address the identified computational capacity limitations. Finally, it is suggested to conduct studies comparing the effectiveness of different control approaches across various aircraft platforms to identify the most versatile and effective methods under diverse operational conditions.

Author contributions

The authors contributing to the study played specific roles in the development of the autopilot control system for aircraft lateral/directional dynamics. Carlos SÁNCHEZ was in charge of the analysis, design and optimization of the control system, while Andrés ORTEGA supervised the analysis and validation of the mathematical model. Mildred CAJAS led the integration, validation and analysis of study results, while Paola CALVOPIÑA focused on the simulation of the control system using tools such as Matlab/Simulink. These individual contributions were crucial to the successful development of the study and the effective implementation of the autopilot control system on the aircraft.

References

Afonso, F., Sohst, M., Diogo, C. M. A., Rodrigues, S. S., Ferreira, A., Ribeiro, I., Marques, R., Rego, F. F. C., Sohouli, A., Portugal-Pereira, J., Policarpo, H., Soares, B., Ferreira, B., Fernandes, E. C., Lau, F., & Suleman, A. (2023). Strategies towards a more sustainable aviation: A systematic review. *Progress in Aerospace Sciences*, *137*, Article 100878. https://doi.org/10.1016/j.paerosci.2022.100878

Aishwarya, C. (2022). The Instrument Landing System (ILS) – A review. *International Journal of Progressive Research in Science and Engineering*, *3*(03), 1–6. https://journal.ijprse.com/index.php/ijprse/article/view/507

Alabsi, M., & Fields, T. (2018). Flight controller learning based on real-time model estimation of a quadrotor aircraft. *Proceedings of the Institution of Mechanical Engineers*, *Part G: Journal of Aerospace Engineering*, *233*(9), 3298–3312. https://doi.org/10.1177/0954410018795524

American Institute of Aeronautics and Astronautics. (2000). *Flight control systems*. AIAA. https://doi.org/10.2514/4.866555

Azeez, M. I., Abdelhaleem, A. M. M., Elnaggar, S., Moustafa, K. A. F., & Atia, K. R. (2023). Optimization of PID trajectory tracking controller for a 3-DOF robotic manipulator using enhanced Artificial Bee Colony algorithm. *Scientific Reports*, *13*, Article 11164. https://doi.org/10.1038/s41598-023-37895-3

Benevides, J., Paiva, M., Simplicio, P., Inoue, R., & Terra, M. (2022). Disturbance observer-based robust control of a quadrotor subject to parametric uncertainties and wind disturbance. *IEEE Access*, *10*, 7554–7565. https://doi.org/10.1109/ACCESS.2022.3141939

Cavanini, L., Ippoliti, G., & Camacho, E. F. (2021). Model predictive control for a linear parameter varying model of an UAV. *Journal of Intelligent and Robotic Systems: Theory and Applications*, *101*(3), 1–18. https://doi.org/10.1007/s10846-021-01337-x

Coello, L. A., Jácome, F. A., Zurita, J. R., Casa, C. W., & Vélez, J. S. (2023). Design and simulation of an aircraft autopilot control system: Longitudinal dynamics. In *Lecture notes in networks and systems. Trends in Artificial intelligence and computer engineering* (LNNS, Vol. 619, pp. 388–402). Springer. https://doi.org/10.1007/978-3-031-25942-5_31

Collinson, R. P. G. (2023). Autopilots and flight management systems. In *Introduction to avionics systems* (pp. 259–284). Springer. https://doi.org/10.1007/978-3-031-29215-6_8

Cook, M. V. (2013). Flight dynamics principles: A linear systems approach to aircraft stability and control. In *Flight dynamics principles: A linear systems approach to aircraft stability and control* (pp. 1–575). Elsevier. https://doi.org/10.1016/C2010-0-65889-5

Cortez, B., Peter, F., Lausenhammer, T., Oliveira, P., Author, F., & Lisboa, T. (2020). *Reinforcement learning for robust missile autopilot design* (arxiv). Cornell University. https://arxiv.org/abs/2011.12956v2

Dudek, E., & Kozłowski, M. (2018). The concept of the instrument landing system – ILS continuity risk analysis method. *Communications in Computer and Information Science*, *897*, 305–319. https://doi.org/10.1007/978-3-319-97955-7_21

Elbatal, A., Youssef, A. M., & Elkhatib, M. M. (2021). Smart aerosonde UAV longitudinal flight control system based on genetic algorithm. *Bulletin of Electrical Engineering and Informatics*, *10*(5), 2433–2441. https://doi.org/10.11591/eei.v10i5.2342

Elsisi, M., Altius, M., Su, S. F., & Su, C. L. (2023). Robust Kalman filter for position estimation of automated guided vehicles under cyberattacks. *IEEE Transactions on Instrumentation and Measurement*, *72*. https://doi.org/10.1109/TIM.2023.3250285

Elsisi, M., Zaini, H. G., Mahmoud, K., Bergies, S., & Ghoneim, S. S. M. (2021). Improvement of trajectory tracking by robot manipulator based on a new co-operative optimization algorithm. *Mathematics*, *9*(24), Article 3231. https://doi.org/10.3390/math9243231

Fu, J., Huang, J., Song, L., & Yang, D. (2020). Experimental study of aircraft achieving dutch roll mode stability without weathercock stability. *International Journal of Aerospace Engineering*, *2020*. https://doi.org/10.1155/2020/8971275

Guardeño, R., López, M. J., & Sánchez, V. M. (2019). MIMO PID controller tuning method for quadrotor based on LQR/LQG theory. *Robotics*, *8*(2), Article 36. https://doi.org/10.3390/robotics8020036

Kashyap, V., & Vepa, R. (2023). Reinforcement learning based linear quadratic regulator for the control of a quadcopter. In *AIAA 2023-0014 Session: International Student Conference – Masters Category*. AIAA. https://doi.org/10.2514/6.2023-0014

Liu, X., & Qin, X. (2020). A probability-based core dandelion guided dandelion algorithm and application to traffic flow prediction. *Engineering Applications of Artificial Intelligence*, *96*, Article 103922. https://doi.org/10.1016/j.engappai.2020.103922

Mo, H., & Farid, G. (2019). Nonlinear and adaptive intelligent control techniques for quadrotor UAV – A survey. *Asian Journal of Control*, *21*(2), 989–1008. https://doi.org/10.1002/asjc.1758

Okyere, E., Bousbaine, A., Poyi, G. T., Joseph, A. K., & Andrade, J. M. (2019). LQR controller design for quad-rotor helicopters. *The Journal of Engineering*, *2019*(17), 4003–4007. https://doi.org/10.1049/joe.2018.8126

Qiao, W., & Wu, S. (2023). The modeling and simulation of turbulence for civil aircraft compliance verification test. *Journal of Physics: Conference Series*, *2658*(1), Article 012056. https://doi.org/10.1088/1742-6596/2658/1/012056

Reis, W. P. N. dos, Couto, G. E., & Junior, O. M. (2023). Automated guided vehicles position control: A systematic literature review. *Journal of Intelligent Manufacturing*, *34*(4), 1483–1545. https://doi.org/10.1007/s10845-021-01893-x

Rodrigues, L. (2021). Affine quadratic optimal control and aerospace applications. *IEEE Transactions on Aerospace and Electronic Systems*, *57*(2), 795–805. https://doi.org/10.1109/TAES.2020.3029625

Sariyildiz, E., & Ohnishi, K. (2015). An adaptive reaction force observer design. *IEEE/ASME Transactions on Mechatronics*, *20*(2), 750–760. https://doi.org/10.1109/TMECH.2014.2321014

Simões, A. M., & Cavalcanti, V. M. G. B. (2023). Missile autopilot design via structured robust linear parameter-varying synthesis. *Journal of Guidanace, Control, and Dynamics, 46*(8), 1649–1656. https://doi.org/10.2514/1.G007580

Sir, A., & Naci, S. (2022). Robust LQR and LQR-PI control strategies based on adaptive weighting matrix selection for a UAV position and attitude tracking control. *Alexandria Engineering Journal*, *61*(8), 6275–6292. https://doi.org/10.1016/j.aej.2021.11.057

Sun, C. T., & Adnan, A. (2021). *Mechanics of aircraft structures*. John Wiley & Sons.

Zhao, S., Zhang, T., Ma, S., & Chen, M. (2022). Dandelion optimizer: A nature-inspired metaheuristic algorithm for engineering applications. *Engineering Applications of Artificial Intelligence*, *114*, Article 105075. https://doi.org/10.1016/j.engappai.2022.105075

Zuo, Z., Liu, C., Han, Q. L., & Song, J. (2022). Unmanned aerial vehicles: Control methods and future challenges. *IEEE/CAA Journal of Automatica Sinica*, *9*(4), 601–614. https://doi.org/10.1109/JAS.2022.105410